The effect of model parameters on the predictions of core-annular flow behavior in a fast-fluidized gas/solids bed

Sofiane Benyahia and Madhava Syamlal
Fluent Incorporated
3647 Collins Ferry Road, Suite A
Morgantown, WV 26505
Ph. (304) 598-5863; Fax (304) 598-7185; E-mail: sof@fluent.com

Thomas J. O'Brien
US Department of Energy
MS-N04, 3610, Collins Ferry Road
Morgantown, WV 26505
Ph. (304) 285-4571, E-mail: tobrie@netl.doe.gov

Abstract

The main purpose of this study is to investigate the ability of three gas-solids flow models – standard granular kinetic theory (see Gidaspow, 1994), and two gas-solids turbulence models (Balzer et al. 1996, and Cao and Ahmadi 1995) – to predict core-annular flow behavior commonly observed in dense gas/solids flows (>3% solids volume fraction). For dense gas/solids flows, these models use similar closures for the solids stresses derived from kinetic theory of granular materials and differ mainly in their treatment of the gas/solids turbulence interchange. The effect of three types of boundary conditions, Jenkins (1997), Johnson and Jackson (1987), and the free slip condition, was also investigated. Care was taken to ensure that the comparisons are based on grid-independent solutions. This study has demonstrated that the granular kinetic theory, Balzer et al. 1996, and Cao and Ahmadi 1995 models give similar predictions for a dense fully developed flow in a vertical channel, and that the gas turbulence may not have a dominant effect in relatively dense gas/solids flows. Finally, the core-annular flow behavior with maximum solids concentration at the walls was not observed if the boundary condition causes production of granular energy at the wall. Boundary conditions that dissipate granular energy near the wall are needed to predict a core-annular flow structure.

Introduction

Experimental investigations of dilute gas/solids flow with high gas/solids velocities, showing a migration of solids toward the core of the flow system, have been widely reported in the literature (Tsuji et al., 1991; Jones and Sinclair, 2003). This phenomenon has been predicted by the use of different gas/solids turbulence models (Balzer et al., 1996; Cao and Ahmadi, 1995; Jones and Sinclair, 2003), which are dominated by the turbulence properties of the carrier gas.

For denser flows, solids migrate towards the walls, establishing a core-annular flow regime. Tsuo and Gidaspow (1990) were probably the first to compute clusters and streamers in the riser section of a circulating fluidized bed. More recently, Agrawal et al. (2001) have conducted a detailed analysis of the formation of clusters and their impact on the gas/solids flow behavior. They computed a large slip velocity between gas and solids that can be several times that of terminal velocity for a single particle. The granular temperature was also computed to be much higher than that of a uniform state due to the large gradients in solids velocity associated with the formation of clusters.

The formulation of the solids pressure, which causes solids migration, is generally agreed upon (Lun et al.,1984; Sinclair and Jackson, 1989; Cao and Ahmadi, 1995; Balzer et al., 1996). However, the models differ in their representation of gas/solids turbulence interaction terms, closure equations for solids viscosity and conductivity, and the drag term. Boundary conditions for the solids granular temperature and slip velocity (Johnson and Jackson, 1987; Jenkins and Louge, 1997; free slip) are another source of variation. We investigate the effects of these differences, using the same numerical code (MFIX) under the same simplified flow conditions. The differences in the predicted granular temperature profiles had a direct impact on the establishment of the core-annular flow.

Description of the models used for gas/solids flow predictions

The model equations for gas/solids flows used in the present study are summarized in Table 1. All the models used in this study, including Simonin model, use solids stresses that are derived from the kinetic theory of granular flows (KTGF) (e.g., Gidaspow 1994). It is reasonable to use KTGF since the simulated gas/solids flows in this study were all conducted at relatively high solids concentrations (3% average solids volume fraction). More details of Ahmadi and Simonin models can be found elsewhere (Cao and Ahmadi, 1995; Balzer et al., 1996; Benyahia et al., 2004). The major differences in these models reside in their treatment of the turbulence exchange terms as shown in Table 1. In this study, we used an algebraic formulation of the gas-particle instantaneous velocity cross-correlation k_{12}, which was found to yield similar results compared with the PDE formulation (Balzer et al. 1996) and yet accelerate significantly the numerical simulations. This algebraic expression was obtained by assuming the dissipation term to be equal to the exchange term in the k_{12} equation (see equation 17 in Benyahia et al., 2004), which is a reasonable assumption since heavy particles (glass beads) are used in this study. Also, unlike Ahmadi and Simonin, who have often used low Reynolds k-epsilon model to describe the gas phase turbulence, we use wall functions and avoid the mesh refinement near a wall boundary necessary to resolve the laminar boundary layer.

We use the boundary conditions for the solids phase developed by Jenkins (1997) and Johnson and Jackson (1987) and a free slip boundary condition to asses the sensitivity of the numerical results to the wall boundary condition.

Continuity equation index m=1 (gas) or 2 (solids).

$$\frac{\partial}{\partial t}(\alpha_m \rho_m) + \frac{\partial}{\partial x_i}(\alpha_m \rho_m U_{mi}) = 0$$

Momentum equation

$$\alpha_m \rho_m \left[\frac{\partial U_{mi}}{\partial t} + U_{mj} \frac{U_{mi}}{\partial x_j} \right] = -\alpha_m \frac{\partial P_1}{\partial x_i} + \frac{\partial \tau_{mij}}{\partial x_j} + I_{lmi} + \alpha_m \rho_m g_i$$

Turbulence modeling in the continuous phase

$$\alpha_1 \rho_1 \left[\frac{\partial k_1}{\partial t} + U_{1j} \frac{\partial k_1}{\partial x_j} \right] = \frac{\partial}{\partial x_i}\left(\alpha_1 \frac{\mu_1^t}{\sigma_k} \frac{\partial k_1}{\partial x_i} \right) + \alpha_1 \tau_{1ij} \frac{\partial U_i}{\partial x_j} + \Pi_{k1} - \alpha_1 \rho_1 \varepsilon_1$$

$$\alpha_1 \rho_1 \left[\frac{\partial \varepsilon_1}{\partial t} + U_{1j} \frac{\partial \varepsilon_1}{\partial x_j} \right] = \frac{\partial}{\partial x_i}\left(\alpha_1 \frac{\mu_1^t}{\sigma_\varepsilon} \frac{\partial \varepsilon_1}{\partial x_i} \right) + \alpha_1 \frac{\varepsilon_1}{k_1}\left(C_{1\varepsilon} \tau_{1ij} \frac{\partial U_i}{\partial x_j} - \rho_1 C_{2\varepsilon} \varepsilon_1 \right) + \Pi_{\varepsilon 1}$$

Turbulence modeling of the dispersed phase $\Theta_s = \frac{2}{3} k_2$

$$\alpha_2 \rho_2 \left[\frac{\partial k_2}{\partial t} + U_{2j} \frac{\partial k_2}{\partial x_j} \right] = \frac{\partial}{\partial x_i}\left(\alpha_2 \rho_2 K_2^t \frac{\partial k_2}{\partial x_i} \right) + \alpha_2 \rho_2 \tau_{2ij} \frac{\partial U_{2i}}{\partial x_j} + \Pi_{k2} - \alpha_2 \rho_2 \varepsilon_2$$

Stress tensor

$$\tau_{mij} = 2 \nu_m^t S_{mij} - \frac{2}{3}\delta_{ij}\left(k_m + \nu_m^t \frac{\partial U_{mk}}{\partial x_k} \right)$$

Gas/solids momentum interchange term

$$I_{lmi} = \beta(u_{li} - u_{mi}), \; \beta = \frac{3}{4} C_D \frac{\rho_g \alpha_1 \alpha_2 |u_l - u_m|}{d_p} \alpha_1^{-2.65}, \; C_D = \begin{cases} 24/\mathrm{Re}\left(1 + 0.15\,\mathrm{Re}^{0.687}\right), & \mathrm{Re} < 1000 \\ 0.44, & \mathrm{Re} \geq 1000 \end{cases}$$

Solids pressure

$$P_2 = \frac{2}{3}\alpha_2 \rho_2 k_2 \left[1 + 2\alpha_2 g_0 (1+e)\right], \; g_0 = \left[1 - \left(\frac{\alpha_2}{\alpha_2^{\max}} \right)^{1/3} \right]^{-1}$$

Solids shear and bulk viscosity

$$\nu_2^t = \nu_2^{kin} + \nu_2^{col}, \; \lambda_2 = 5/3\, \nu_2^{col}, \; \nu_2^{kin} = 2/3\left(k_2\left(1 + \zeta_c \alpha_2 g_0\right)\right)\tau_c, \; \nu_2^{col} = 4/5\, \alpha_2 g_0 (1+e)\left(\nu_2^{kin} + d_p \sqrt{\frac{2k_2}{3\pi}} \right)$$

Solids granular conductivity

$$K_2^t = K_2^{kin} + K_2^{col}, \; K_2^{kin} = 2/3\left(k_2\left(1 + \varpi_c \alpha_2 g_0\right)\right)\tau_2^c, \; K_2^{col} = 6/5\, \alpha_2 g_0 (1+e)\left(K_2^{kin} + 5/9 d_p \sqrt{\frac{2k_2}{3\pi}} \right), \; \varpi_c = \frac{(1+e)^2 (2e-1)}{100}$$

Granular model	**Ahmadi model**	**Simonin model**
$\nu_g^t = \nu_g^{laminar}$ $\Pi_{k2} = 0$	$\nu_g^t = \frac{0.09 k_1^2/\varepsilon_1}{1 + \frac{\tau_{12}^x}{\tau_1}\left(\frac{\alpha_2}{\alpha_2^{\max}}\right)^3}$ $\Pi_{k1} = 2\beta(k_2 - k_1)$ $\Pi_{\varepsilon 1} = 0$ $\Pi_{k2} = 2\beta\left(\frac{k_1}{1 + \tau_{12}^x/\tau_1} - k_2\right)$	$\nu_g^t = \frac{0.09 k_1^2/\varepsilon_1}{1 + 0.314 X_{12} \frac{\tau_{12}^x}{\tau_1} / (1 - k_{12}/2k_1)}$ $\Pi_{k1} = X_{12}\beta(k_{12} - 2k_1)$ $\Pi_{\varepsilon 1} = 1.2(\varepsilon_1/k_1)\Pi_{k1}$ $\Pi_{k2} = \beta(k_{12} - 2k_2)$ $k_{12} = \frac{2\,\tau_{12}^t/\tau_{12}^x}{1 + (1 + X_{12})\tau_{12}^t/\tau_{12}^x}(k_1 + X_{12}k_2)$ $X_{12} = \frac{\alpha_2 \rho_2}{\alpha_1 \rho_1}$

Table 1 Model equations for multiphase flows

Gas-phase wall boundary conditions for turbulent flows

$$\left.\frac{\partial U_1}{\partial x}\right|_w = \frac{\rho_1 \kappa U_1 C_{1\mu}^{1/4} k_1^{1/2}}{\left(\mu_1 + \mu_1^t\right)\ln\left(E\,x^*\right)}, \quad x^* = \frac{\rho_1 C_{1\mu}^{1/4} k_1^{1/2} \Delta x/2}{\mu_1}$$

$$\left.\frac{\partial k_1}{\partial x}\right|_w = 0 \;, \; \left.\frac{\partial \varepsilon_1}{\partial x}\right|_w = 0$$

$$k_1 \;\; production\Big|_{at\,fluid\;cells\;next\;to\;wall} = \alpha_1\,\tau_{1ij}\frac{\partial U_i}{\partial x_j} + \beta_{12}\;k_{12} = \alpha_1 \rho_1 \sqrt{C_{1\mu}}\,k_1 \frac{U_1}{\Delta x/2\ln\left(E\,x^*\right)}$$

$$k_1 \;\; dissipation\Big|_{at\;\;fluid\;cells\;next\;to\;wall} = \alpha_1 \rho_1 \varepsilon_1$$

$$\varepsilon_1\Big|_{at\;\;fluid\;cells\;next\;to\;walls} = \frac{C_{1\mu}^{3/4} k_1^{3/2}}{\kappa \Delta y/2}$$

Johnson and Jackson boundary condition for the solids phase

$$\left.\nu_2^t \frac{\partial V_s}{\partial x}\right|_w + \frac{\phi\pi\, V_s g_0 \sqrt{2/3\,k_2}}{2\sqrt{3}\;\alpha_2^{\max}} = 0$$

$$\left.K_2^t \frac{\partial k_2}{\partial x}\right|_w - \frac{\phi\pi\, V_s^2 g_0 \sqrt{2/3\,k_2}}{2\sqrt{3}\;\alpha_2^{\max}} + \frac{\sqrt{3}\pi\;g_0\left(1-e_w^2\right)\left(2/3\,k_2\right)^{3/2}}{4\,\alpha_2^{\max}} = 0$$

Jenkins and Louge small frictional limit

$$S^{sf}\big/N^{sf} = \mu \;, \; \frac{Q^{sf}}{N^{sf}\left(3\Theta_s\right)} = \frac{3}{8}\left[\frac{7}{2}\left(1+e_w\right)\mu^2 - \left(1-e_w\right)\right]$$

Free slip boundary condition

$$\left.\frac{\partial V_s}{\partial x}\right|_w = 0\,, \; \left.\frac{\partial \Theta_s}{\partial x}\right|_w = 0\,, \; \left.\frac{\partial V_g}{\partial x}\right|_w = 0$$

Table 2 Model boundary conditions for multiphase flows

Description of physical and numerical parameters

We report the simulation results for the isothermal flow of air and glass beads in a vertical channel of 10 cm width. A superficial gas velocity of 5 m/s and an average solids volume fraction of 3% are used in all these simulations unless otherwise specified. A constant gas mass flux was prescribed in these simulations. The gas pressure drop was allowed to fluctuate in order to guaranty a constant gas flow rate. The glass beads used in these simulations had a diameter of 120 microns and density of 2.4 g/cm^3. Particle-particle restitution coefficient of 0.95 and particle-wall coefficient of 0.7 were used. In most of the simulations, the Jenkins low frictional limit was used as the solids phase boundary condition with a particle-wall friction coefficient value of 0.2. Uniformly distributed computational grids have been used in this study with a standard grid of 40 cells along the channel width. Second order discretization scheme of Van Leer was used for the convective terms. The numerical time step was allowed to vary but rarely exceeded a millisecond.

Verification study of model predictions and grid convergence

A recent paper by John Grace (2004) has focused on the shortcomings of current models used for the predictions of gas/solids flows. More specifically, the paper points out the lack of verification studies. Although verification is invariably a part of numerical model development, it seldom gets reported. For example, the research code MFIX used in this study is verified with a suite of 35 test cases every time a stable version of the code is created. Commercial CFD codes are rigorously tested using a large number of test cases. We start this paper by reporting on a test case we used specifically for this study to test the implementation of the granular theory model.

In a recent study Gidaspow (2003) derived a closed form solution for the granular temperature radial profile, in the case where solids velocity has a parabolic profile (Poiseuille flow):

$$V_s = 3/2\ V_s^{avg} \left[1 - \left((X - H)/H\right)^2\right]$$

In this case, the granular temperature has a fourth power dependency on the dimensionless channel width as shown by the following equation:

$$\Theta_s = 2\, V_s^{avg}\ \frac{\mu_s}{\lambda_s} \left[1 - \left((X - H)/H\right)^4\right].$$

In order to verify the numerical code in MFIX, a simulation was conducted after prescribing the granular temperature to be the fourth power profile (Figure 1-b). The results of the simulation are shown in Figure 1. Figure 1-c shows an exact match between the analytical and numerical solutions for solids velocity. Figure 1-a shows the predicted solids volume fraction profile and a function proportional to the inverse of granular temperature. An exact inverse relationship between the granular temperature and the solids volume fraction can be deduced from the radial momentum balance. These exact matches partially verifies the kinetic theory expressions coded in MFIX. (Although not relevant to this verification test, for reference Figure 1-b also shows the granular temperature profile predicted using kinetic theory, which does not compare well with the prescribed granular temperature profile.) Figure 1-a also shows that in the case where the full solids pressure is used (kinetic and dense parts) the solids volume fraction was lower near the walls of the channel. The core-annular flow behavior with higher solids concentration near the walls of the channel is always observed when the highest granular temperature occurs at the center of the channel.

The difference between the predicted gas and solids axial velocity (Figure 1-c) matches exactly the terminal velocity of a single glass bead particle estimated at about 80 cm/s. We will demonstrate later that the slip velocity between gas and solids can be several times that of a single particle terminal velocity due to cluster formation. In this case, clusters did not form because the imposed granular temperature profile forced the code to produce steady (time invariant) results.

A grid sensitivity analysis was conducted in the periodic 1-D channel to determine the minimum computational grid size needed to achieve a grid independent solution. Several grid densities were considered in this study varying from a relatively coarse mesh of 10 grids distributed along the channel width to a finer mesh of 160 grids. Figure 2 shows that a grid density of 40 along the channel width was necessary to achieve grid independent time-averaged results. Although the coarse grid of 10 cells was able to predict the core-annular flow, the numerical predictions of other variables are not accurate as demonstrated by Figure 2.

One-dimensional versus two-dimensional clusters and their effect on flow predictions

Two-dimensional simulations have been carried out in a channel of 10 cm width and 40 cm height with a uniform computational grid of 40x160. The choice of a length to width ratio of four has been found to produce optimal results (Agrawal et al., 2001). Figure 3-a shows the solids volume fraction distribution along the width of the channel at an elevation half that of the total height. The 2-D simulation predicted a core-annular flow similar to the 1-D simulation. However, the solids concentration at the walls of the channel was less in the case of a 2-D simulation. The clusters and streamers (sheets of high solids concentration) formed in the 2-D channel and followed a complex path in their fall due to gravity. Although most clusters and streamers remained near the walls of the channel, some clusters moved to the center of the channel. This was demonstrated by the relatively smaller concentration of solids near the walls and higher concentration of solids in the center of the riser in the 2-D simulations compared to the 1-D results.

The computed granular temperature in a 2-D system was lower than that in the 1-D case as seen in Figure 3-b. The relatively smaller clusters computed near the channel walls in the 2-D case lead to a smaller downward velocity, which in turn yielded smaller solids velocity gradients that are the main mechanism for granular temperature production.

Figure 3-c shows a comparison of the computed gas axial velocity profiles between 1-D and 2-D results. The average gas velocity was fixed in both cases to 5 m/s, thus the profiles for 1-D and 2-D systems were similar except near the walls where the 1-D simulation predicted a larger downward velocity due to entrainment by the larger computed clusters.
The 2-D results showed higher solids velocity magnitude relative to 1-D simulation as seen in Figure 3-d. The 2-D shape of clusters makes them more susceptible to entrainment by the upward flowing gas. A better exchange of momentum is achieved in a 2-D cluster relatively to a 1-D cluster that extends infinitely in the axial direction. For these reasons, the 2-D solids velocity profiles were higher in magnitude relative to the 1-D results. However, the trends and magnitude of all the computed results were similar in both 1-D and 2-D simulations. These results suggest that using a 1-D system to study the effect of model parameters and boundary conditions is acceptable. One should point out that the 1-D results may not compare well with experiments; however, the purpose of this study is to compare the different turbulence models and boundary conditions.

Effect of gas/solids turbulence models on the flow predictions

Three different models were used to predict the gas/solids flow in a one-dimensional channel: a standard kinetic theory model (KTGF) with no dissipation or production of granular temperature due to drag terms (see Gidaspow, 1994); Simonin model (Balzer et al., 1996); and Ahmadi (Cao and Ahmadi, 1995) model. For the heavy particles at high solids loading used in these simulations, the three models had differences only in the gas/solids turbulence interaction terms. Simonin and Ahmadi models predicted similar granular stresses as the standard KTGF model.

Figure 4-a shows that all three models predicted similar solids volume fraction distributions. The core-annular behavior was predicted due to the transient fluctuations in the solids volume fraction. Animations of the solids volume fraction showed that all models predicted an oscillatory behavior with a period of 6-7 sec. This oscillatory behavior created clusters that moved from one wall of the channel to the other. When averaged over time, the solids volume fraction distribution showed a core-annular behavior with solids concentration higher at the walls of the channel. The dissipation in the granular temperature equation due to inelastic collisions or interactions with the gas turbulence in the cases of Simonin or Ahmadi models did not affect the core-annular behavior predicted by all these models. A previous study by Sinclair and Jackson (1989) using a steady-state model has shown an undue sensitivity of their model to the particle-particle restitution coefficient. Another study by Hrenya and Sinclair (1997) demonstrated the limitations of a steady state model and re-derived a Reynolds-averaged model with proposed closures to the generated correlations. Their model explained the nature of core-annular behavior that is due to the formation of clusters, which is a transient phenomenon that can be captured by the standard model based on the kinetic theory of granular flow with a sufficiently fine computational grid.

Figure 4-b shows the gas and solids time-averaged turbulent kinetic energy distribution along the channel width ($k_2 = 3/2\,\Theta_s$). The predicted granular temperature was the highest in the case of a granular model due to the absence of gas/solids turbulence exchange term in the granular temperature equation. Simonin model predicted a higher granular temperature due to the low predictions of the gas turbulent energy. Ahmadi model predicted similar magnitude and profiles of gas and solids turbulent energy. The high magnitude of the gas turbulent energy predicted by Ahmadi model was due to the high production turbulence exchange term in the k_1 equation. There was a slight increase in the gas turbulent energy near the walls in both Ahmadi and Simonin models due to the use of standard wall functions.

Figure 4-c shows the time-averaged gas axial velocity profile along the channel width. Simonin and Ahmadi models along with the laminar model predicted the same gas velocity profile even when the gas turbulent kinetic energy was significantly different in both profile and magnitude. This is a clear indication that the gas turbulence model does not play a significant role in dense (3% averaged solids volume fraction) flows. It also indicates that a model based only on the kinetic theory for granular flows is sufficient to model gas/solids flows in relatively dense systems. The transient dense flow of gas and solids indicates that the gas flow through regions of minimum solids concentration. The presence of highly concentrated regions (or clusters) prohibits the high velocity flow of gas. Thus, the gas velocity profile is affected mainly by the solids volume fraction profile and not by the gas turbulent energy distribution, as in single-phase flows.

Figure 4-d shows the time-averaged solids axial velocity profiles along the10-cm channel width. Solids flow downward near the walls of the channel because of the high solids concentration in these regions. At the center of the channel, where solids concentrations are low, the highest solids velocity is observed. This is typical of a core-annular flow behavior commonly observed in experiments. The difference between gas and solids axial velocity was computed to be several times that of a single particle terminal velocity, which is approximately equal to 80 cm/s. This was due to the formation of clusters that can accelerate downward at a speed higher than that of a single particle, which is in agreement with the observations of Agrawal et al. (2001).

Effect of different boundary conditions for the solids stresses on flow predictions

Three different boundary conditions were used in this study: Jenkins and Louge (1997) small frictional limit, Johnson and Jackson (1987) boundary condition commonly used for gas/solids flows, and the free slip boundary condition. Apart from the parameters described in the physical and numerical section in this study, the Jenkins boundary condition used a friction coefficient (μ) equal to 0.2, and a specularity coefficient (ϕ) of 0.01 was used with the Johnson and Jackson boundary condition.

Figure 5 shows the predictions of the granular model using different wall boundary conditions for the solids stresses as summarized in Table 2. Both the free slip and Jenkins boundary conditions (BC) predict maximum solids concentration at the walls of the channel. However, Johnson and Jackson BC predicts a thicker annulus and the maximum solids concentration occurred at a small distance from the walls. This was caused by the fact that the minimum granular temperature occurred at a location close to the walls. In fact, Figure 5-b shows that the Johnson and Jackson BC predicted a small production of granular temperature at the walls. By further increasing the specularity coefficient to 0.1, we did not observe the presence of the core-annular flow behavior and the code predicted a steady flow with maximum solids volume fraction away from the wall region. The same behavior was observed by using a higher friction coefficient (μ) in the Jenkins BC. In fact, by using a friction coefficient of 0.25, we did not observe a core-annular behavior, which was similar to the results observed using Johnson and Jackson BC with a high specularity coefficient. To explain the reason for this change in behavior, let's examine the Jenkins BC for granular temperature: $\frac{Q^{sf}}{N^{sf}(3\Theta_s)} = \frac{3}{8}\left[\frac{7}{2}(1+e_w)\mu^2 - (1-e_w)\right]$. This boundary condition will yield a production of the granular temperature at the walls only if $7/2(1+e_w)\mu^2 > (1-e_w)$. When the particle-wall restitution coefficient is 0.7, this analysis shows that for a value of the friction coefficient higher than about 0.22, a production of granular temperature occurs at the walls. This indicates that a core-annular flow behavior will form if the walls dissipate granular temperature, thus demonstrating the significance of boundary conditions and their effect on the model predictions.

Figure 5-d shows the solids axial velocity predictions using different wall boundary conditions. The larger the wall-particle friction, the lower the solids slip velocity computed at the walls. In this case, the Johnson and Jackson BC had the largest friction as seen in Figure 5-d. The gas is usually entrained with the solids even near a wall boundary as seen

in Figure 5-c. Therefore, different wall boundary conditions for the gas phase may not be important in dictating the overall gas/solids flow patterns due to the lower inertia of the gas in dense systems. Figure 5-d shows also that most solids downward flow occurs with the free slip condition due to the lack of wall friction that tends to slow the downward flow of large clusters.

Conclusions

The verification of the granular model in MFIX was conducted by using a closed form solution of the granular temperature derived by Gidaspow (2003); it was verified that by fixing the granular temperature profile, the numerical and analytical solutions for the solids velocity matched exactly. A series of simulations were conducted with increasing grid refinement to select a grid size that gives grid-independent, time-averaged solutions.

The comparison of different turbulence models and boundary conditions was done by conducting several transient 1-D simulations, which are useful for comparing models because they are considerably faster than 2-D or 3-D simulations. A few 2-D simulations were also conducted to test the validity of comparisons based on 1-D simulations. A major difficulty with 1-D simulation is that the size of the clusters in the flow directions is infinite, and, therefore, their downward velocity near the wall is larger than that predicted by a 2-D simulation. Nevertheless, the solids velocity profiles predicted by 1-D and 2-D simulations agreed qualitatively. There was good quantitative agreement in predicted solids volume fraction and gas velocity profiles.

Three gas/solids models have been examined to study a relatively dense (3% solids by volume) gas/solids fully-developed and transient flow. For dense gas/solids flows, these models use similar closures for the solids stresses derived from kinetic theory of granular materials and differ mainly in their treatment of the gas/solids turbulence interchange. This study has demonstrated that the granular kinetic theory, Balzer et al. 1996, and Cao and Ahmadi 1995 models give similar predictions for a dense fully developed flow in a vertical channel, and that the gas turbulence may not have a dominant effect in relatively dense gas/solids flows.

Finally, the core-annular flow behavior with the maximum solids concentration at the walls was not observed if the boundary condition causes production of granular energy at the wall. Boundary conditions that dissipate granular energy near the wall are needed to predict a core-annular flow structure.

References

Agrawal, K., Loezos, P.N., Syamlal, M and Sundaresan, S., 2001. The Role of Meso-Scale Structures in Rapid Gas-Solid Flows, J. Fluid. Mech., 445, 151-185.

Benyahia, S., Syamlal, M. and O’Brien, T.J., 2004. Evaluation of Boundary Conditions used to Model Dilute, Turbulent Gas/Solids Flows in a Pipe. Submitted for publication in *Powder Technology*.

Balzer, G., Simonin, O., Boelle, A. and Lavieville, J., 1996. A unifying modelling approach for the numerical prediction of dilute and dense gas-solid two phase flow, CFB5, *5th Int. Conf. on Circulating Fluidized Beds*, Beijing, China.

Cao, J. and Ahmadi, G., 1995. Gas-particle two-phase turbulent flow in a vertical duct. *Int. J. Multiphase Flow*, Vol. 21 No. 6, pp. 1203-1228.

Gidaspow, D. (2003), Hydrodynamics of fluidization using kinetic theory: An emerging paradigm?, in Recent Res. Devel. Chemical Eng., Transworld Research Network, Trivandrum, India, Vol 5, 53-81.

Gidaspow, D., 1994. Multiphase Flow and Fluidization: Continuum and Kinetic Theory Description. Academic Press.

Grace, J.R. and Taghipour, F., 2004. Verification and validation of CFD models and dynamic similarity for fluidized beds. Powder Technology, vol. 139, pp. 99-110.

Hrenya, C.M., and Sinclair, J.L, 1997, Effects of particulate-phase turbulence in gas-solids flows, AIChE J., 42, 853-869.

Jenkins, J.T. and Louge, M.Y., 1997. On the Flux of Fluctuating Energy in a Collisional Grain Flow at a Flat Frictional Wall, *Phys. Fluids* 9 (10), pp. 2835-2840.

Johnson, P.C. and Jackson, R., 1987. Frictional-Collisional Constitutive Relations for Granular materials, with Application to Plane Shearing. *J. Fluid Mech.*, 176, 67-93.

Jones, N.E. and Sinclair, J.L., 2003. Effect of Solids Loading in Dilute and Dense Gas-Solid Flow, to be published in *AIChE J*.

Lun, C.K.K., Savage, S.B., Jeffrey, D.J. and Chepurniy, N., 1984. Kinetic theories of granular flows: inelastic particles in Couette flow and slightly inelastic particles in a general flow field. J. Fluid Mech., Vol. 140, pp. 223-256.

Simonin, O., 1996. “Continuum modeling of dispersed two-phase flows, in Combustion and Turbulence in Two-Phase Flows, Von Karman Institute of Fluid Dynamics Lecture Series 1996-2.

Sinclair, J.L. and Jackson, R., 1989. Gas-Particle Flow in a Vertical Pipe with Particle-Particle Interactions, *AICHE J.*, **35(9)**, 1473-1486.

Tanaka, T. and Tsuji, Y., 1991. Numerical Simulation of Gas-Solid Two-Phase in a Vertical Pipe: on the Effect of Inter-Particle Collision, in *4th Symposium on Gas-Solid Flows*, ASME FED, Vol. 121, 123-128.

Tsuo, Y.P. and Gidaspow, D., 1990. Computation of flow patterns in circulating fluidized beds. *AICHE J.*, Vol. 36, pp. 964-970.

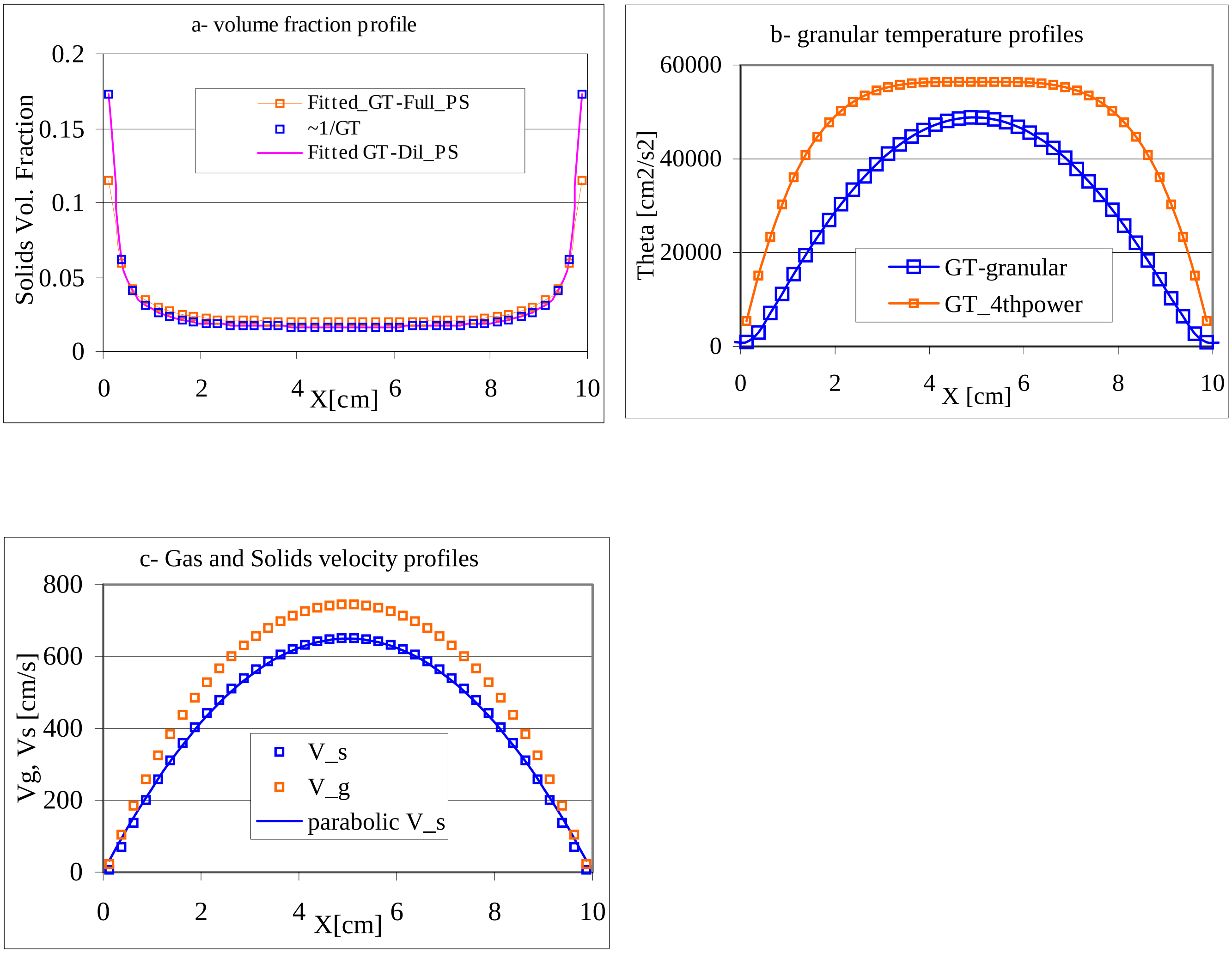

FIGURE 1. Verification of the numerical implementation of the granular model in MFIX by imposing a theoretically derived granular temperature profile.

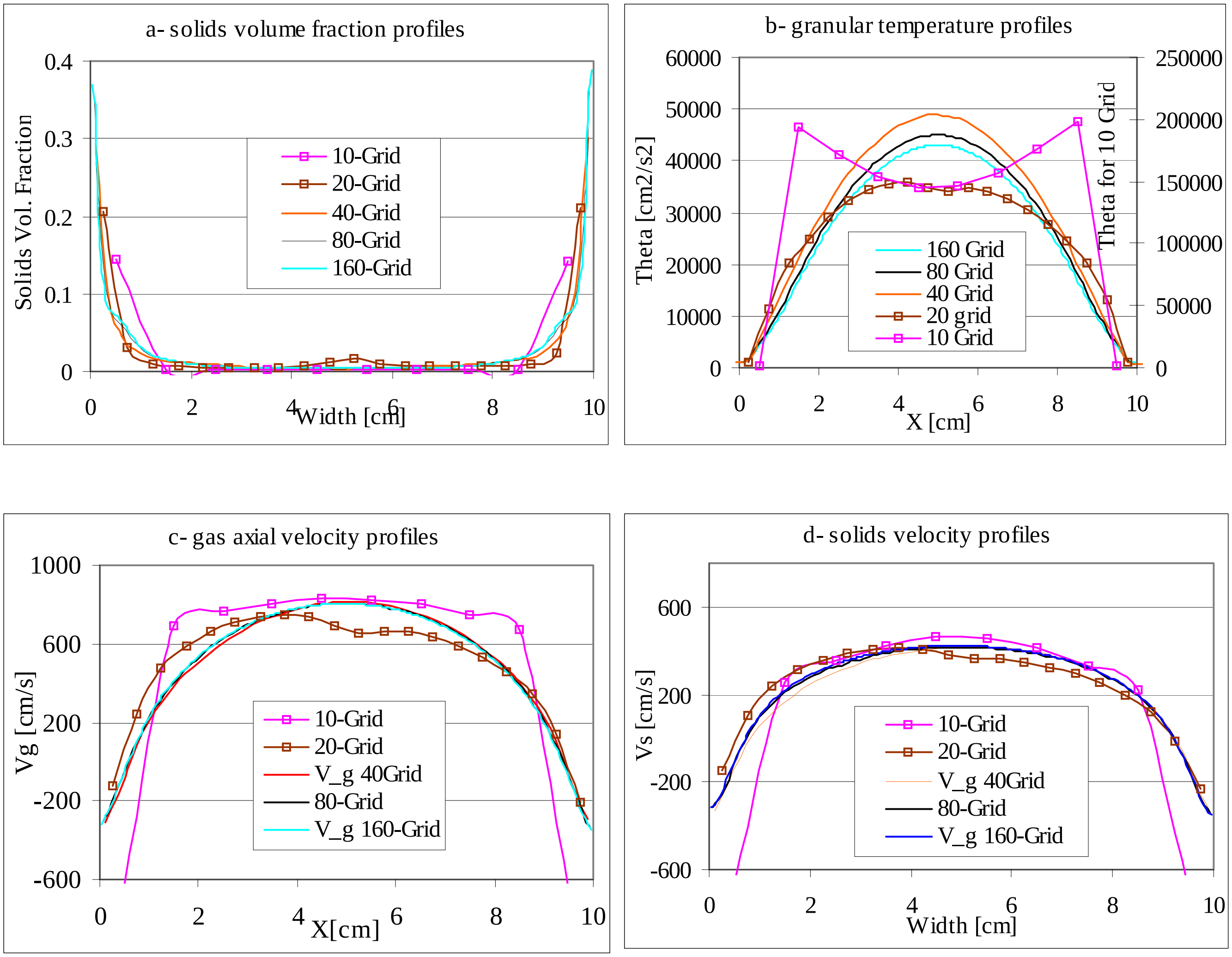

FIGURE 2. Grid sensitivity analysis of the time-averaged flow variables conducted in a one-dimensional fully developed channel.

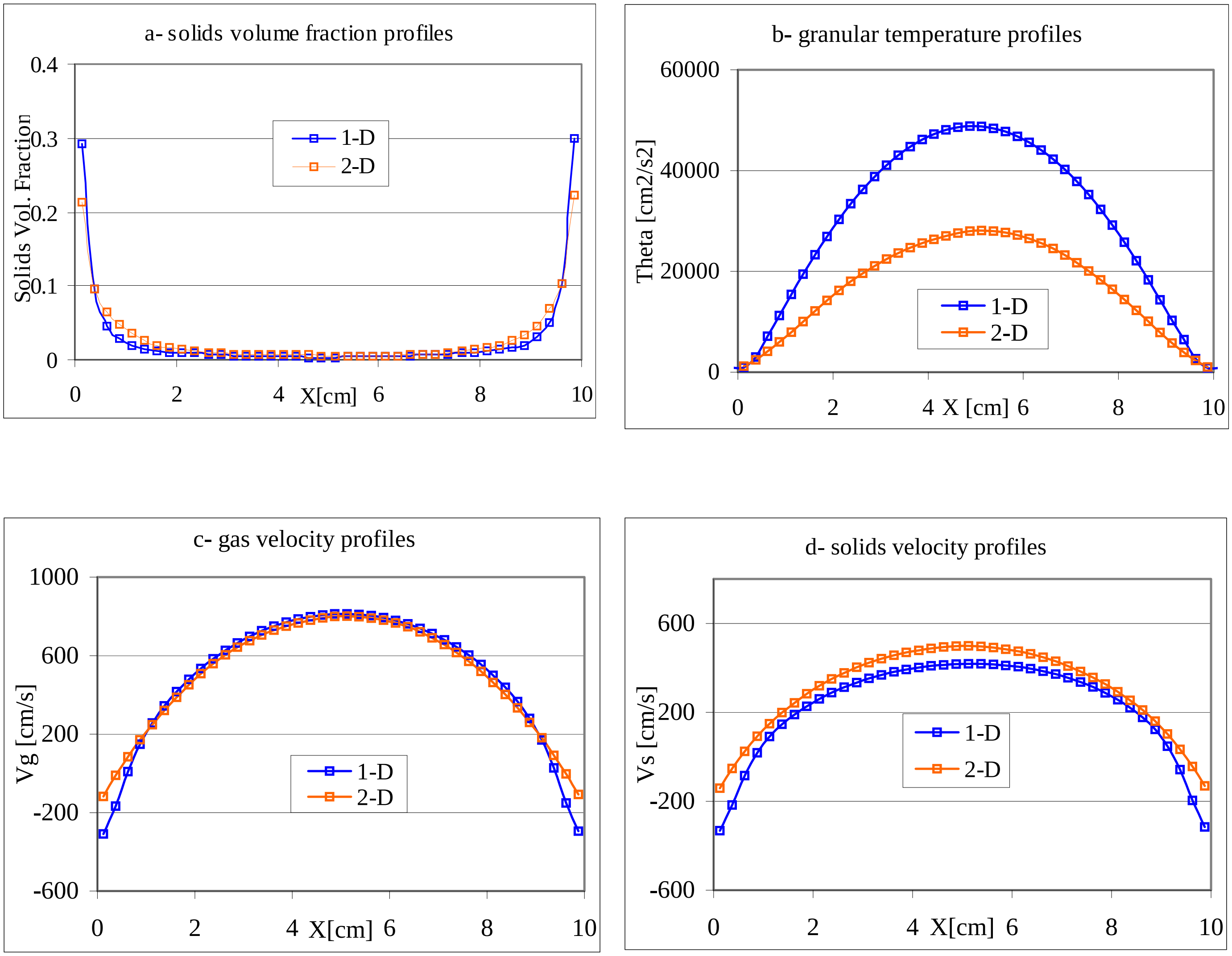

FIGURE 3. Comparison of the one-dimensional versus two-dimensional flow predictions in a fully developed channel.

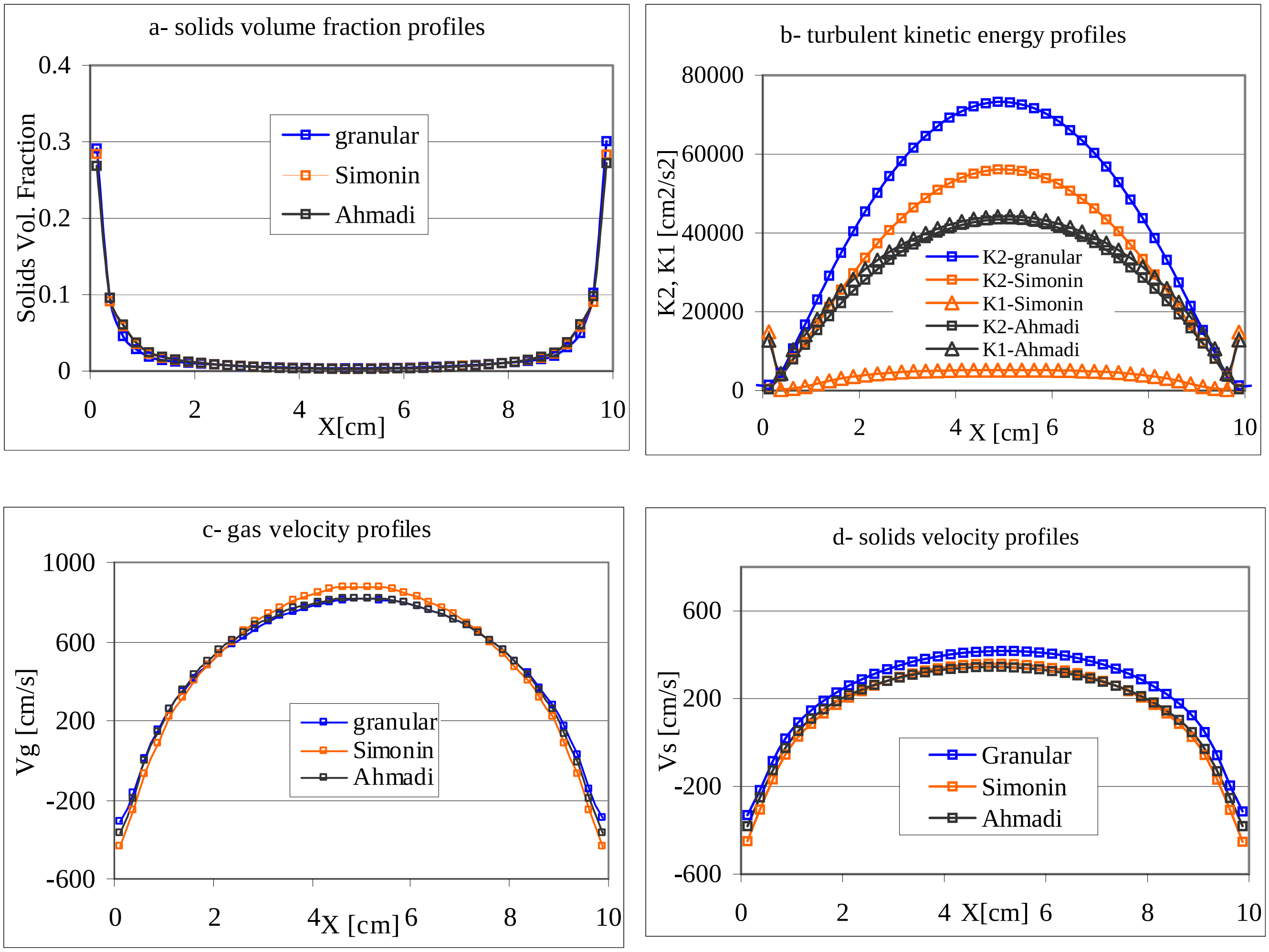

FIGURE 4. Effect of using different gas/solids turbulence models on the flow predictions in a one-dimensional fully developed channel.

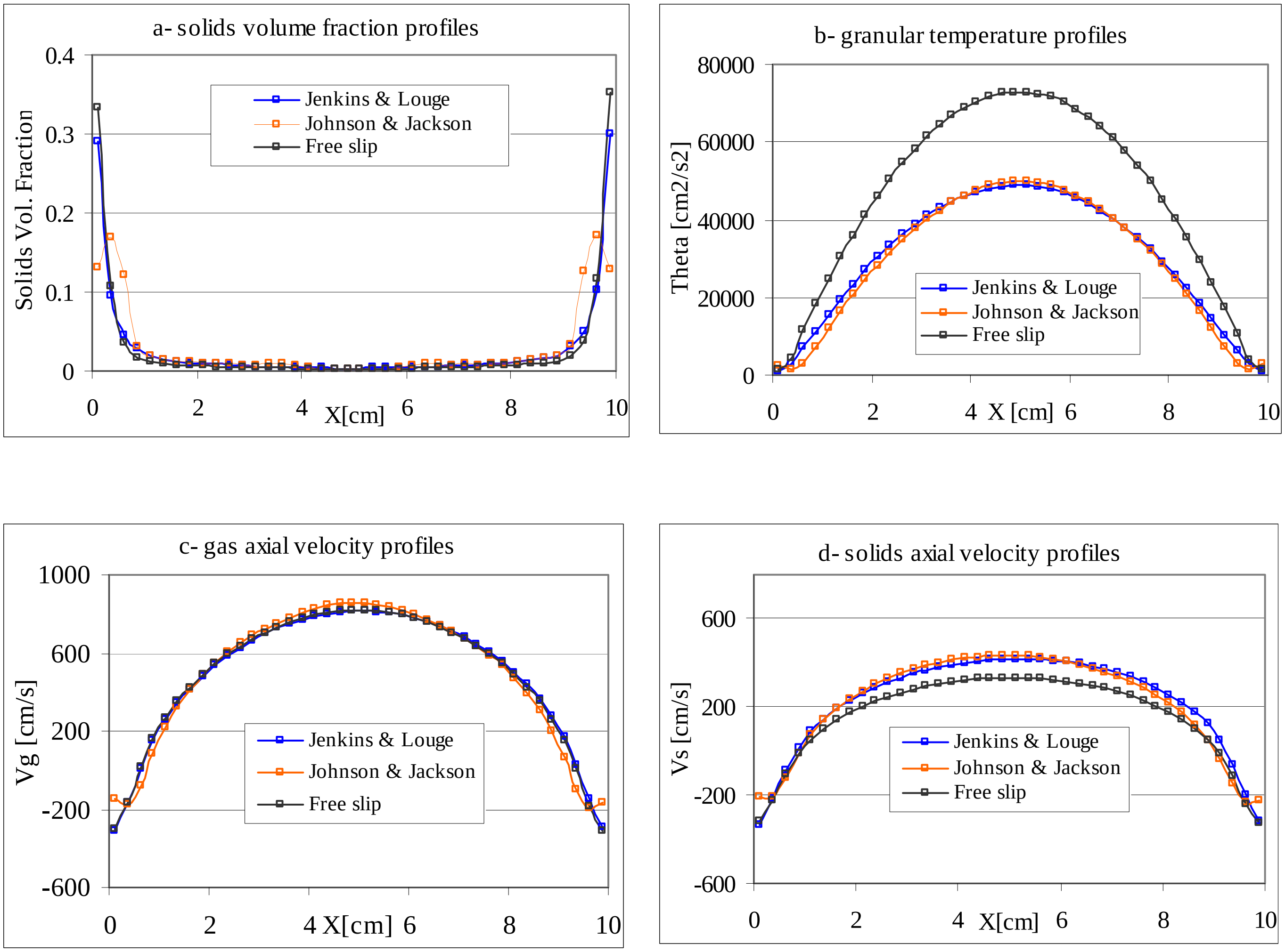

FIGURE 5. Effect of using different wall boundary conditions for the solids stresses on the time-averaged flow variables.